Journal of the European Ceramic Society **18** (1998) 1025–1036

PII: S0955-2219(98)00006-5
0955-2219/98/$19.00 + 0.00

Particle Formation Paths in the Synthesis of Silicon Nitride Powder in a Laser-Heated Aerosol Reactor

Frank Einar Kruis,* Wim Oostra, Jan Marijnissen, Joop Schoonman and Brian Scarlett

Department of Chemical Engineering and Department of Inorganic Chemistry, Delft University of Technology, Julianalaan 136, 2628 BL Delft, The Netherlands

(Received 4 October 1996; accepted 19 December 1997)

Abstract

The Laser-chemical vapour precipitation of Si_3N_4 powder by reacting SiH_4 and NH_3 was studied using a newly developed laminar gas mixing system. Thermophoretic sampling enabled monitoring of the formation process on a milli-second basis and shows the existence of two synthesis paths: the nitridation of Si particles and the sintering of directly formed Si_3N_4. The latter route leads to almost stoichiometric α- and β-Si_3N_4, with particle sizes up to 150 nm. The Si_3N_4 particles do not decompose above the thermodynamic decomposition temperature, probably due to kinetic reasons since the residence time is of the order of milliseconds. © *1998 Elsevier Science Limited. All rights reserved*

1 Introduction

Silicon nitride ceramics have been extensively studied for high-temperature structural applications, especially for application to ceramic engine components. This is mainly due to their large strength over a wide temperature range, good thermal shock resistance and strong wear and corrosion resistance. However, pure silicon nitride is very difficult to sinter, mainly due to the volatiliy and small diffusivity of Si and N. Liquid forming sintering aids improve the density of the sintered product but at the expense of the strength at high temperature and incurring a higher cost of the finished parts. High-purity and submicron powders should be ideal for sintering.[1]

*To whom correspondence should be addressed at Process and Aerosol Measurement Technology, Gerhard-Mercator-Universität, Duisburg, Bismarckstr. 81, 47057 Duisburg, Germany.

Powder control is very important in controlling the quality of ceramics. The larger the surface area the greater the driving force for sintering and thus there is a requirement for powders with high surface area. Also important for sinterability are void space, which should be as small as possible, and the number of particle contacts per unit volume.[2] It is clear that agglomeration of the particles also reduces the sinterability of a powder because of the packing problem. This can lead to micro-cracks in the sintered material.

Si_3N_4 powders are prepared by direct nitridation of silicon or silicide, carbothermic reduction of silica, decomposition of silicon dimide and by vapour-phase reactions, e.g. between silanes and ammonia. Currently, two methods are thought to satisfy all the requirements for a high-quality Si_3N_4 powder:[3] thermal decomposition of silicon diimide and gas-phase synthesis using silane, SiH_4, as the silicon source and ammonia as the nitrogen source. The resultant powders are usually submicron in size, but often contain excess silicon. Prochazka and Greskovich[4] prepared amorphous, cream-coloured Si_3N_4 powders with a composition close to the stoichiometry of Si_3N_4 at a molar ratio of the input gases, NH_3 and SiH_4, greater than 10. The powders crystallized to α-Si_3N_4 after thermal treatment at 1750 K. Janiga *et al.*[3] showed that the amount of free Si decreases with increasing ratio of NH_3 to SiH_4, and is minimal at a ratio of twelve. Powders prepared at 1670 K contained some α-Si_3N_4 but the powders prepared at lower temperatures were amorphous.

This research was based on the synthesis of Si_3N_4 using laser-chemical vapour precipitation (L-CVP). In this process a CO_2 laser is used as a heat source for the gas-phase reaction:

$$3\,SiH_4 + 4\,NH_3 \rightarrow Si_3N_4 + 12\,H_2 \qquad (1)$$

The SiH_4 molecules are known to absorb the infrared laser radiation emitted by CO_2 lasers with a wavelength around 10·6 μm. The characteristics of this process, developed by Haggerty *et al.*[5,6] are a well-defined reaction zone in a cold-wall reactor, very short residence times, of the order of milliseconds, high-purity products due to the absence of contaminating surfaces and good energy-efficiency. Several researchers have used the L-CVP process to synthesize Si_3N_4. Important parameters appeared to be: (1) the reactants, (2) the ratio of the silicon to nitrogen reactant, and (3) the way in which the reactants are mixed. Silane is in most cases used as the silicon reactant but it has been shown that cheaper chlorinated silanes can also be used.[7] The molar ratio of NH_3 and SiH_4 is mostly between 5 and 20. In the case of a NH_3–SiH_2Cl_2 reaction ratios as low as 2 were applied.[7] In most set-ups, the reactants are premixed[5,6] but it was shown that the primary particle size can be increased from smaller than 20 nm to more than 100 nm by injection of the ammonia into the reaction zone.[8] In that case, it is supposed that silicon particles are first formed and then subsequently nitrided.

One of the main problems of the L-CVP process is the difficulty of obtaining stoichiometric powders: silicon is easily co-precipitated resulting in a nitrogen-content lower than the stoichiometric value of 39·9 w/w%, which is deleterious to its sinterability. Another problem is the particle size, which ideally should be between 100 nm and 1 μm. Most researchers report smaller particles, of the order of 10 to 30 nm. Finally, the powders produced tend to be amorphous or only partially crystalline, and require additional processing to obtain crystalline powder. Using the injection-type reactor,[8] crystalline silicon nitride was obtained directly, thus suggesting the necessity for more research on the mixing of the reactants.

For work presented here, a new reactor design was used and optimized for the synthesis of silicon nitride, permitting controlled mixing of the SiH_4 and NH_3. The synthesis of silicon particles is first described, not only because of its promising role as starting powder in the production of reaction bhonded silicon nitride (RBSN), but also in order to understand better the formation processes taking place in the laser-heated flame. The particle formation process was investigated experimentally using a specially developed device to extract samples from different places in the reaction zone. The different possible formation processes in the synthesis of Si_3N_4, with their consequences for powder characteristics, will be illustrated.

2 Experimental Procedure

2.1 Reactants

Silane, SiH_4, (99·999%, Air Products Nederland B.V., Waddinxveen, The Netherlands) and ammonia, NH_3 (99·999%, Air Products) were used as reactants for synthesis of silicon nitride. The carrier and sheath gas, N_2, and the dilution gas, H_2, were purified using a commercially available oxygen and moisture absorber (Chrompack, Frankfurt, Germany).

2.2 Laser-CVP with laminar coaxial mixing-type reactor

The importance of controlled mixing of the SiH_4 and the NH_3 is shown already on the basis of phase diagrams. Another requirement is that the mixing be laminar. This facilitates the experimental observations, the *in-situ* sampling and temperature measurements and avoids turbulent deposition of the particles onto the windows through which the laser enters and leaves the reactor. This extends the possible run-time of a synthesis. The newly developed laminar coaxial mixing system enables the controlled mixing of the reactants without inducing turbulence. This mixing system consists of four concentric nozzles directing the flow of the gases. The source gas, here the SiH_4, and the reactant, the NH_3, flow from the first and third nozzle, respectively. These flows are prevented from mixing with each other too early by means of the inert 'sheath' gas, here N_2, flowing from the second nozzle. The gases exiting the nozzles cross the laser beam orthogonally which is located about 2 mm above the nozzle system. Absorption of the laser beam by the SiH_4 results in a hot reaction zone, visible in the form of a flame. The reaction products are created in this zone and are carried away by a stream of N_2 gas flowing from the fourth, large diameter (8 mm inner diameter) nozzle. The nozzles were constructed from stainless-steel. The small dimensions of the nozzles, inner diameter 0·7, 1·4, and 2·4 mm, required a special construction in order to enable them to be removed individually and in order to obtain a configuration in which all the needles are correctly centered. Each of the needles was mounted on a larger holder which fitted onto a screw tapping into the reactor base.

A schematic drawing of the complete reactor system is shown in Fig. 1. A tunable, 200-W continuous CO_2 laser (Edinburgh Instruments PL6, Edinburgh, UK), radiating at a wavelength of 10·60 μm (the 10P20 line) was focussed with a ZnSe lens with a focal length of 30 cm to a spot 1·5 mm in diameter centered 2·0 mm above the inner nozzle. The laser entered and left the stainless-steel reactor system through windows of ZnSe,

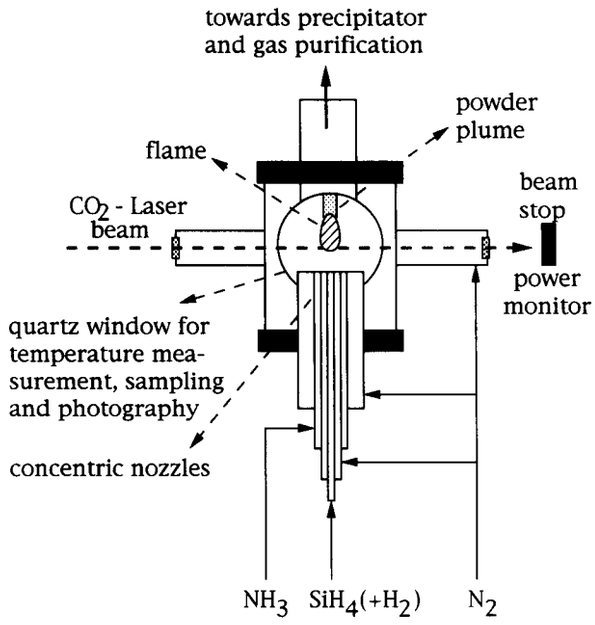

Fig. 1. Schematic drawing (not on scale) of the L-CVP reactor with the laminar coaxial mixing system.

located at the end of two small tubes in order to limit possible particle deposition and consequent burning of the windows. Absorption by the lens and the windows reduces the laser power to about 150 W. Two quartz windows of large diameter (10 cm) in the reactor enable visual observation of the flame and also temperature measurements by means of a two-color pyrometer.[7] In order to be able to change the position of the laser beam, the whole reactor was mounted on a movable table. The gas and particle stream exiting from the flame flowed through a tubular funnel to stabilize the flame and was connected to an electrostatic collector operating between 5 and 10 kV and 0·2 to 0·5 mA. The pyrex collection tube could be closed by two large valves and brought into a glove box without oxidation of the powder. Possible unreacted SiH_4 was removed in a furnace mounted after the collection system. All the experiments were carried out at atmospheric pressure but using a valve and a pump system the reactor could be evacuated in order to remove the air after the system has been exposed to air. The gas control system consisted of a series of mass flow controllers (MKS Instruments 1259B and 147B, Delft, The Netherlands) and safety valves coupled to a pressure transducer (MKS Instruments) and an emergency button. The gas flasks were placed in a cabinet (Air Products Nederland B.V., Waddinxveen, The Netherlands) for safety reasons.

In order to produce silicon in this reactor, SiH_4 flowed from the first nozzle surrounded by a low-velocity N_2 stream. In the case of synthesis of Si_3N_4, the configuration used all the four nozzles. Starting from the central nozzle the SiH_4, the N_2 as a sheath gas, the NH_3, and the N_2 carrier gas were metered, respectively. The gas flows were such that the velocities of the SiH_4, the N_2, and the NH_3 were approximately equal [80 $cm^3 min^{-1}$ at standard conditions (sccm) SiH_4, 160 sccm N_2 and 320 sccm NH_3].

All the powders synthesized were handled in a glove box filled with argon and free of water and oxygen. The particle size and morphology were determined by using a transmission electron microscope (Philips EM400, Eindhoven, The Netherlands) and by BET surface area determination. The powders were analyzed using IR spectroscopy and X-ray diffraction with a diffractometer (Model D500, Siemens, Germany) operated at 45 kV and 30 mA. The nitrogen content of the powders was determined by decomposing the samples into LiOH at 950 K and then measuring the amount of NH_3 released by a conduction technique.[7]

2.3 Thermophoretic sampling to investigate particle formation in the reaction zone

In general, two methods are used for the experimental investigation of particle formation in flames. Light scattering methods are able to determine particle size and number concentration and have already been applied to a similar system.[9] The main problems are that the refractive index of the particles, which is a function of temperature and composition, should be known and that non-uniformities along the axis of sight can severely hinder scattering experiments. The other technique is thermophoretic sampling which has been used in research on soot formation[10] and silica formation.[11] In this technique, a cold surface is moved through the flame and the particles are captured on the surface because of the thermophoretic force. This force acts in the direction of decreasing temperature, as the particles are bombarded by higher energy molecules on the high temperature side and are driven towards the lower temperature region. The advantage of this technique is that the morphology of the particles captured can be characterized, and that chemical and crystallographic methods can be applied to the particles.

The use of thermophoretic sampling in the L-CVP reactor must overcome specific problems such as the small dimensions of the flame, the high temperatures, the extremely high number concentrations of the particles and the closed high purity gas reactor system. In addition, the particles must be captured onto a standard TEM grid because of the nanometer size scale of the particles. A device was constructed which consists of a pneumatically controlled probe holding a small tube with a slide at the end where a rectangular

TEM grid, reduced to 1×3 mm, can be held with a small screw. In this way the TEM grid can be moved quickly through the flame while the probe moves along the flame (Fig. 2). Stroboscopic lighting in combination with photography showed the velocity of the sampling arm to be around 0·1 m s^{-1}. In order to avoid exposure to the air, the sampling apparatus was fitted in a chamber separated from the reactor system by a large gate-valve and connected to a vacuum-pump and a nitrogen purge. The vertical and horizontal position of the probe could be changed in order to take samples from different positions from the flame and could be recorded using photography. The whole device was connected to the reactor by removing one of the two large quartz windows.

The particles depositing on the grid should, of course, be representative of those present at a certain position in the flame. Because the particles are very small, different sized particles have the same thermophoretic deposition efficiency because for these particles thermophoresis is independent of particle size.[12] Another demand to be met is that the deposition mechanism be only thermophoretic and not turbulent or inertial, which mechanisms are size-dependent. Turbulent deposition takes place when the Reynolds number of the flow around the grid is greater than unity:[13]

$$\mathrm{Re} = \rho_g v L/\eta > 1 \qquad (2)$$

Here ρ_g is the viscosity of the gas, v the velocity, L the characteristic length of the obstacle and η the viscosity of the gas. Calculation of this Reynolds number, using the gas properties of H_2 at 2000 K, a gas velocity of 5 m s^{-1} and a characteristic length of the grid of 1 mm, revealed a Reynolds number of 0·5. Thus turbulent deposition will not play an important role. Inertial deposition occurs when the ratio of the stopping distance of the particle and characteristic dimension of the obstacle is smaller than unity. This is the Stokes' number. The stopping distance D_s is given by Hinds[13] as:

$$D_s = \rho_p d_p^2 C_c v/18\eta \qquad (3)$$

Here ρ_p is the particle density, d_p the particle diameter and C_c the slip correction factor (20 for a 10 nm particle and 3 for a 100 nm particle). The stopping distance for a particle of 10 nm in H_2 at 2000 K moving with a velocity of 5 m s^{-1} is 10 nm and is 200 nm for a 100 nm particle, indicating that the particle will follow the stream line of the gas very closely. Inertial impaction will thus play no role in particle deposition.

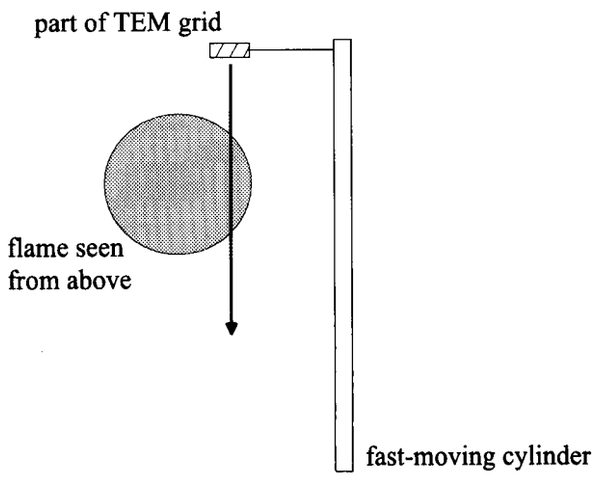

Fig. 2. Schematics of the thermophoretic sampling apparatus to extract particles from the flame on a TEM grid.

3 Results and Discussion

3.1 Silicon synthesis

When the SiH_4 flowing from the inner nozzle is heated with the laser beam, a stable luminescent flame with a base of 2·5 mm in diameter is formed. Two-colour pyrometry revealed that the centreline temperature increases sharply up to 2000 K and then gradually decreases (Fig. 3), which is visually seen as a decrease in luminescence. The slightly higher temperatures when using a sheath gas flow of N_2 around the SiH_4 flow is probably due to a more confined flow of the inner SiH_4 flow induced by the sheath gas. When SiH_2Cl_2 was used as the reactant, a maximum temperature of 1550 K was

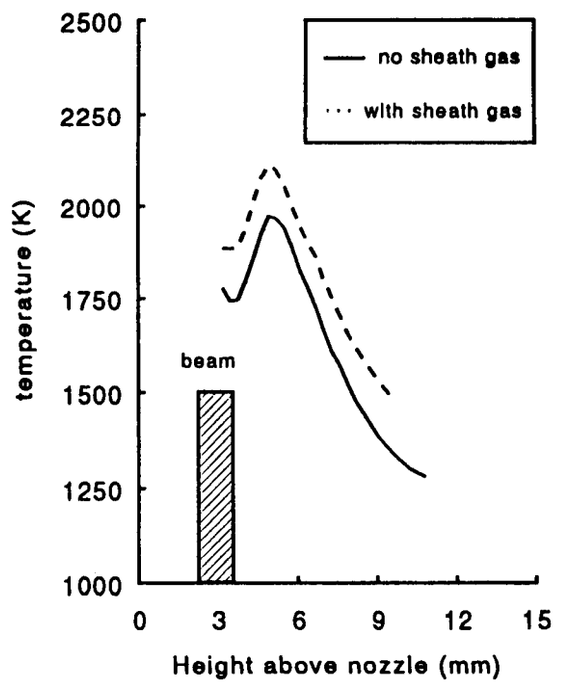

Fig. 3. Centreline temperature as a function of the height above the nozzle for the SiH_4 flame (100 sccm SiH_4, sheath gas 200 sccm N_2).

attained.[7] This lower temperature probably occurred because the decomposition reaction of SiH_2Cl_2 is more endothermic than that of SiH_4. Considering the lateral temperature distribution at one height in the flame, two maxima are observed at the meeting point of the laser beam and the gases at a position 0·8 mm off the centreline, but, 2 mm higher in the flame a temperature maximum is observed at the centreline while at the visual flame boundary a temperature lower by 500 K was observed. The reason for the lower temperature at the boundary is the dilution by the surrounding N_2 gas. The occurrence of the temperature maxima low in the flame can be explained by the velocity profile of the silane gas emerging from the nozzle, with the maximum velocity at the centre according to the laminar parabolic profile characteristic for tubular flow. When the velocity is higher, the residence time in the laser beam is shorter and, therefore, also the heating of the gas and particles is smaller, leading to the off-centered temperature maxima. Another reason for the velocity difference is the heating of the gas, which causes a volume increase, especially in the centre.

The particle formation process was investigated using the sampling apparatus. Samples taken from the position in the flame where the temperature is at its maximum (2000 K) show spherical, crystalline silicon particles with particle diameters between 35 and 70 nm. The particles appear to have been deposited below the melting point of silicon due to the cooling in the boundary layer around the grid since individual overlapping particles can be discerned. There is also a small number of agglomerates of smaller primary particles, 10–30 nm. These particles show sinter necks and no overlap. Samples taken higher in the flame at lower temperature, about 1350 K, contain particles which are more agglomerated and in which sintering has clearly taken place, now also in the case of the larger particles. The number of primary particles per agglomerate has clearly increased and the polydispersity decreased. The agglomerates of smaller, primary particles are also still present. Samples taken above the flame show no clear difference to those from the middle sample point except that there are almost no agglomerates of relatively few primary particles. In most cases the primary particles in an agglomerate are approximately of the same size. A simple monodisperse model can describe the number-reducing aggregation process. The surface-is also reduced, either due to coalescence above the melting point or sintering below the melting point. This model predicts the evolution of the particle size, particle aggregation and number concentration with time and position.[14] According to this model, even below the melting point of Si (1680 K), characteristic for the outer boundaries of the flame, the sintering mechanism can result in primary particles of 30 nm. They then become, however, more aggregated than at higher temperatures.

3.2 Silicon synthesis: effect of residence time

In order to produce larger particles, a larger inner nozzle diameter (2·4 mm) was used together with the same volumetric gas flow, resulting in a lower velocity and a higher residence time. A mixture of perfectly spherical Si particles, up to several hundreds of nanometres in diameter, together with smaller, more aggregated and sintered particles was found. This is, again, thought to be due to the temperature profile over the width of the flame. The large, unsintered particles have been in the center of the flame and above the melting point long enough to reach a size where the characteristic sintering time is smaller than the residence time. The neck growth rate of a 10 nm particle is 10^4 times as fast as a 100 nm particle according to a model based on grain-boundary diffusion.[14] Therefore the smaller particles sinter much faster and are thus more susceptible to undesired agglomerate formation. Experiments in which samples were taken from the visual boundaries of the flame, where lower temperatures and concentrations prevailed, showed small, agglomerated particles whilst the large, spherical particles were absent. It can, therefore, be concluded that the large particles are formed by coagulation above the melting point of silicon attaining a size where sintering is too slow to be of importance. The small, agglomerated particles are formed by aggregation and sintering below the melting point at the outer boundaries of the flame.

3.3 Si_3N_4 synthesis

The controlled synthesis of Si_3N_4 is of interest because the formation mechanisms are not yet fully understood. A better understanding would facilitate the commercial exploitation of the system. In order to characterize the L-CVP reactor, three process variables were varied: (1) dilution of the SiH_4 with H_2, (2) the flow rate of the sheath gas, and thereby the mixing between SiH_4 and NH_3, and (3) the diameter of the laser beam.

The intended laminar mixing flame appeared indeed not to be turbulent and to be very stable. There was no particle deposition in the reactor. In comparison to the SiH_4 decomposition flame, the SiH_4/NH_3 flame is brighter and has a whiter colour. This is in accordance with the temperature measurements, which showed higher temperatures when NH_3 was added, even as high as 3000 K in some cases (Fig. 4). It must be observed that Si_3N_4

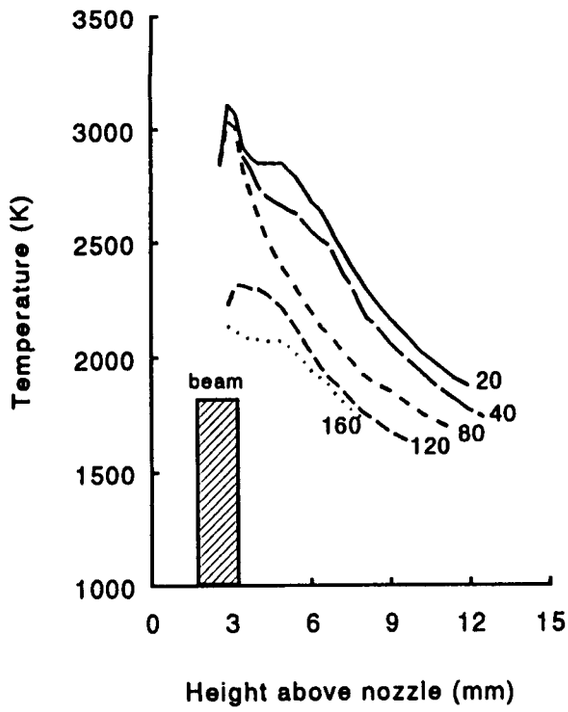

Fig. 4. Centreline temperature as a function of the height above the nozzle for the $SiH_4/N_2/NH_3$ system with the flow of the sheath-gas N_2 indicated in sccm.

is thermodynamically unstable at the conditions in this study above about 2000 K where it decomposes into Si and H_2.[15] The higher temperatures might be caused by absorption by the Si_3N_4 particles.[7] The NH_3 absorbs also the 10P20 laser radiation. A luminous zone could be seen when the NH_3 was heated in the absence of the SiH_4. Decreasing the sheath gas flow, the N_2 flowing between the SiH_4 and the NH_3, had the most profound effect of the three process variables examined. The lower the sheath gas flow, the higher was the temperature. Two questions arise from these measurements and will be dealt with: (1) why does the sheath gas flow has such a profound influence on the temperature and (2) can particles at temperatures far above the decomposition temperature exist?

Crystallinity, specific surface area and stoichiometry of the powder are the main characteristics of the powders produced. The stoichiometry of the powders can be expressed in terms of the nitrogen-content, which is 40 w/w% for stoichiometric Si_3N_4. The colour is also an indication: pure Si_3N_4 is white, while free Si included into the powder leads to yellow, cream-coloured or tan powder. The specific surface area can be used as an indication of the particle size.

3.4 Effect of H_2 dilution

The first series of runs, using a relatively high sheath-gas velocity, resulted in a yellow-brown powder with a nitrogen content below 20%. Decreasing the concentration of SiH_4 in H_2 increased the specific surface area, as shown in Fig. 5. This can be explained by the lower silicon concentration and the consequent decreased number of collisions which results in a smaller particle size and thus a higher specific surface area. The Si_3N_4 formation proceeds via nitridation of Si, because the high sheath gas velocity prevents fast mixing between the SiH_4 and NH_3. This results in a higher nitrogen content, as is also found experimentally, because smaller Si particles are more easily nitrided, as is shown later in this paper.

3.5 Effect of sheath-gas flow

Decreasing the sheath-gas flow results in a lower specific surface area, as shown in Fig. 6. This is probably due to the transition from the production of Si_3N_4 by nitridation to direct formation from the gas-phase. This is also indicated by the higher nitrogen content. The lower sheath-gas flow results in faster mixing of the SiH_4 and NH_3 and hence contact lower in the flame, maybe even below the flame. The Si_3N_4 particles thus formed can decrease their surface area by sintering mechanisms. The higher the temperature the faster the sintering and this explains the decreasing surface area with decreasing sheath-gas flow. The higher temperatures can be explained by the fact that the Si_3N_4 particles absorb the laser radiation and are thus heated whilst Si particles do not absorb this wavelength.[7] The colour of the powders changes from tan-coloured to yellow-cream and a nitrogen-content of 35 w/w% is reached. It seems thus that a

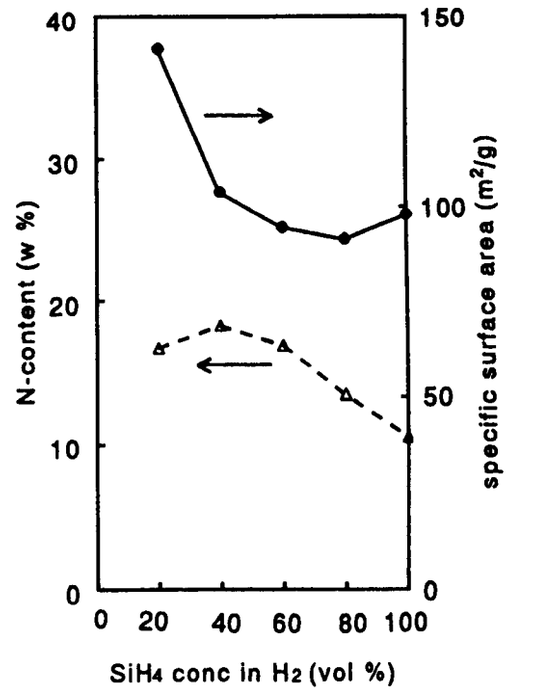

Fig. 5. Nitrogen-content and specific surface area as a function of SiH_4 volume % in H_2 (100 sccm SiH_4+H_2, 200 sccm N_2 sheath-gas, 320 sccm NH_3).

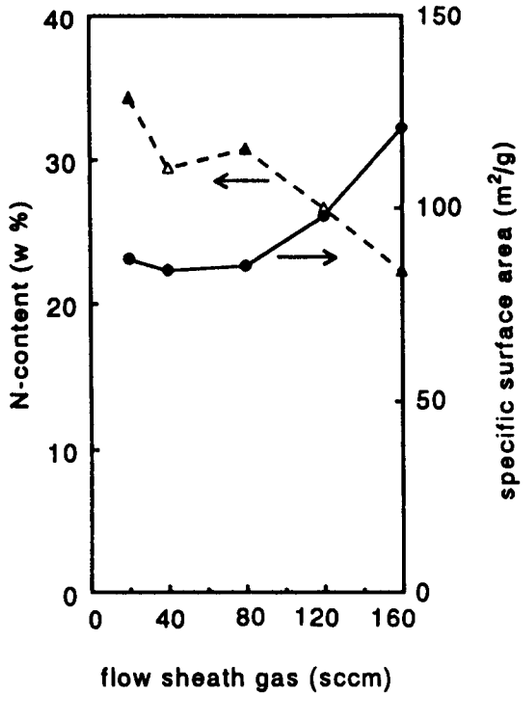

Fig. 6. Nitrogen-content and specific surface area as a function of the flow rate of N_2 sheath-gas (80 sccm SiH_4, 320 sccm NH_3).

lower velocity of the sheath-gas improves the stoichiometry. X-ray diffraction patterns obtained for samples in this series of experiments are shown in Fig. 7. High sheath-gas flow rates, 160 and 80 sccm, show strong crystalline Si peaks, while hardly any crystalline Si_3N_4 could be detected. A low sheath-gas flow rate, 20 sccm, decreased the Si (111) peak sharply, whilst some crystalline Si_3N_4 could be detected. The powder synthesized at this low sheath-gas rate has a nitrogen content of 35 w/w% and due to the absence of a strong crystalline peak consists probably mainly of amorphous Si_3N_4.

3.6 Effect of laser beam diameter

The last experimental parameter to be varied produced almost pure, crystalline Si_3N_4. Increasing the diameter of the laser beam and using a low flow rate of the sheath-gas (40 sccm) does not have a marked effect on the surface area, as seen in Fig. 8, but it has a positive effect on the stoichiometry of the Si_3N_4. Using a broad laser beam, 3·5 mm, a white powder with a nitrogen-content of 39·5 w/w% was obtained. A more uniform heating of the reactants, the NH_3 is now also heated, and a decreased beam intensity probably account for this effect. Initially, the laser beam was intended to heat only the SiH_4, but the absorption by the NH_3 seems to contribute to a more uniform heating of the flame. With a laser beam diameter of 1·5 mm, only two small spots of the surrounding NH_3 are heated, visible in the flame as two bright spots of approximately 1 mm thick. This non-uniformity disappears with increasing laser beam diameter. The X-ray diffraction analysis shown in Fig. 9 indicates that the increased laser beam diameter almost totally suppresses the presence of crystalline Si and results in the presence of strong β-Si_3N_4

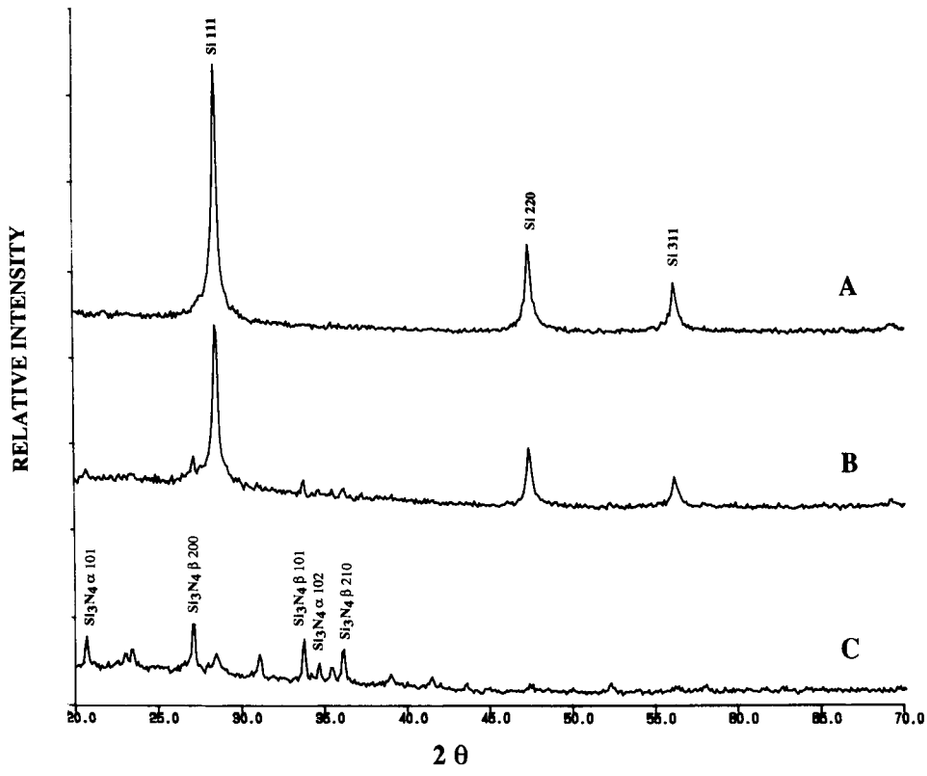

Fig. 7. X-ray diffraction patterns of powders produced with varying sheath-gas flow rate: (A) 160 sccm, (B) 80 sccm and (C) 20 sccm N_2, all with 80 sccm SiH_4 and 320 sccm NH_3.

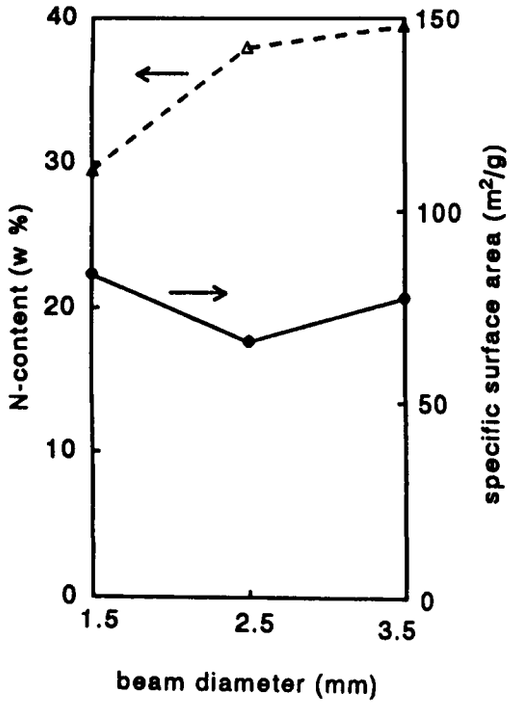

Fig. 8. Nitrogen-content and specific surface area as a function of laser beam diameter (80 sccm SiH_4, 40 sccm N_2 sheath-gas, 320 sccm NH_3).

lines and, to a lesser degree, strong α-Si_3N_4 lines. From these results it seems that crystallization of Si_3N_4 is favoured if it is relatively pure since the temperature profiles of the series with varying laser beam diameter are not markedly different. The powder was investigated with IR-spectroscopy (Fig. 10), which shows a very strong Si–N band around 900 cm^{-1} and peaks characteristic for crystalline Si_3N_4 between 400 and 600 cm^{-1}. Undesired Si–H bonds (2170 cm^{-1}) are not observed, but a small amount of N–H bonds (3340 > cm^{-1}), probably adsorbed NH_3, and a very weak Si–N–H (imide) peak (700 cm^{-1}) can be seen. However, in comparison with other published Si_3N_4 spectra, the powder seems to have a very low content of H and N bonds.

3.7 Powder morphology

The powders produced were studied by TEM. Three kinds of particles could be discerned in almost all of the powders: (1) extremely small, aggregated, amorphous, needle-like particles with diameters between 2 and 4 nm [Fig. 11(a)], (2) amorphous, aggregated, approximately spherical particles with diameters between 10 and 30 nm [Fig. 11(b)], and (3) large, partially crystalline particles of irregular form, often wedge-shaped, with sizes between 30 and 150 nm [Fig. 11(c)]. The only variation of process parameters which had a visible effect was to increase the laser beam diameter. This reduced the number of needle-like [Fig. 11(a)] and aggregated [Fig. 11(b)] particles, but the crystalline particles were more rectangular and edgy [Fig. 11(d)]. Using the X-ray diffraction results, it can be said that these rectangular particles are composed of α- and β-Si_3N_4 while the more rounded, wedge-shaped particles encountered in experiments with a laser beam diameter of 1·5 mm

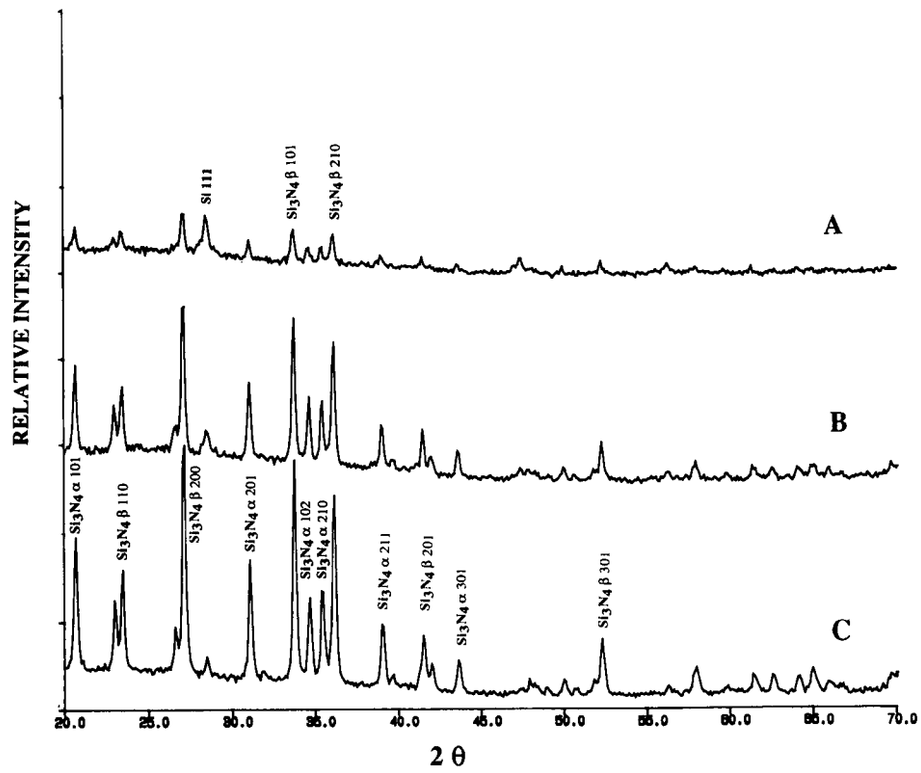

Fig. 9. X-ray diffraction patterns of powders produced with varying laser beam diameter: (A) 1·5 mm, (B) 2·5 mm and (C) 3·5 mm, all with 80 sccm SiH_4, 40 sccm N_2, and 320 sccm NH_3.

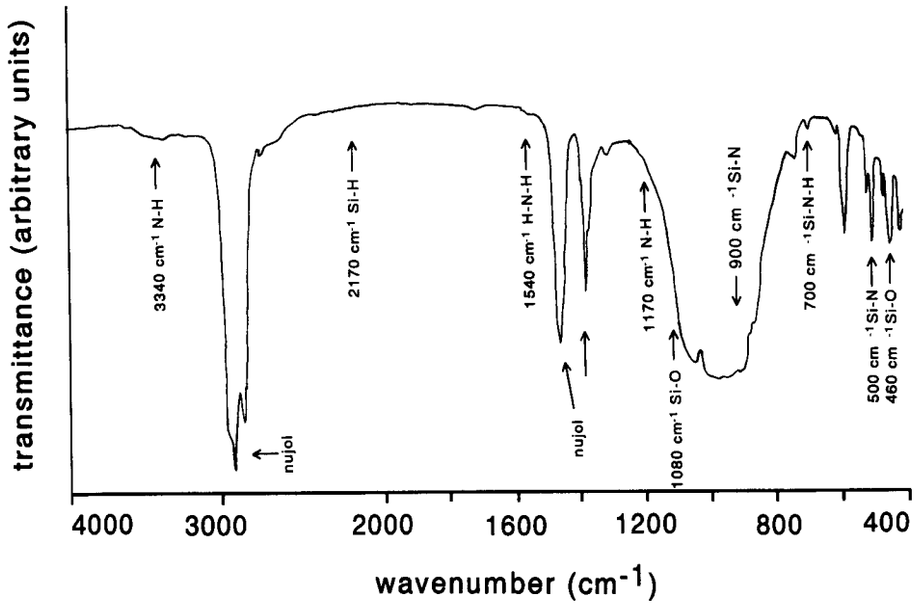

Fig. 10. IR-spectrum of the powder synthesized with 80 sccm SiH_4, 40 sccm N_2, and 320 sccm NH_3, and a laser beam diameter of 3·5 mm.

probably consist of a mixture of crystalline Si and amorphous Si_4N_4. Based on the fact that similar particles are often aggregated and on the non-uniformity of the flame, it is postulated that the different kinds of particles are produced in different parts of the flame and result from concentration and temperature differences. The larger particles originate from the centre of the flame, which the NH_3 reached later and where subsequent Si growth is thus more important, while the smaller, amorphous particles are formed more in the outer regions of the flame as a result of a direct reaction of SiH_4 with NH_3 at lower temperatures. They do not grow by sintering because they flow in the lower-temperature outer boundaries of the flame.

3.8 Experimental confirmation of the existence of different synthesis paths using thermophoretic sampling

In this section it will be shown that thermophoretic sampling, which enables the monitoring of the particle size, morphology and crystallinity on a milli-seconds basis, proves the existence of two different synthesis paths. This was already predicted by thermodynamic considerations, in which the way the phase diagram is traversed is essential for the formation mechanism: via a low-temperature imide precursor, direct formation of Si_3N_4 or via silicon (Fig. 12 in a previous paper[15]). Sampling showed that when operating with a high sheath-gas velocity low in the flame a mixture of spherical, crystalline particles and amorphous, smaller aggregated particles was formed [Fig. 12(a)]. The spherical, overlapping, crystalline particles have the same morphology as particles captured at that place in the flame without NH_3 so they were presumed to be Si. The presence of the smaller, amorphous aggregated particles supports the hypothesis that this class of particles is formed in an early stage of the process by direct contact of SiH_4 and NH_3 at lower temperatures, probably at the outer boundaries of the flame. Higher in the flame and thus some milliseconds later, when the NH_3 reaches the inner flow, the Si is partially transformed into amorphous Si_3N_4, yielding irregular or wedge-shaped particles [Fig. 12(b)]. When using a low sheath-gas velocity and an increased laser beam diameter, small amorphous Si_3N_4 particles were formed low in the flame due to more rapid mixing between the SiH_4 and NH_3 [Fig. 13(a)]. Due to the fact that they are small and amorphous, it was concluded that they are composed of Si_3N_4. Si particles under similar temperatures would have been spherical and much larger. Higher in the flame the particles become larger and some crystallinity develops [Fig. 13(b)]. Above the flame, the rectangular particles of α- and β-Si_3N_4, as shown in Fig. 11(d), must be formed during the cooling of the process stream as they are present in the final product, but could not be detected using sampling from the flame. It is surprising to find Si_3N_4 particles at temperatures above the dissociation temperature, where they should convert to liquid Si according to thermodynamics.[15] The steady development of particle size and morphology in the flame renders sampling artefacts as gas-to-particle conversion in the boundary-layer of the grid improbable. Therefore, it is postulated that once the Si_3N_4 has been formed, the residence time above the decomposition temperature, in the order of 1 ms, is too low to allow decomposition. On the other hand, NH_3 will tend to decompose at these

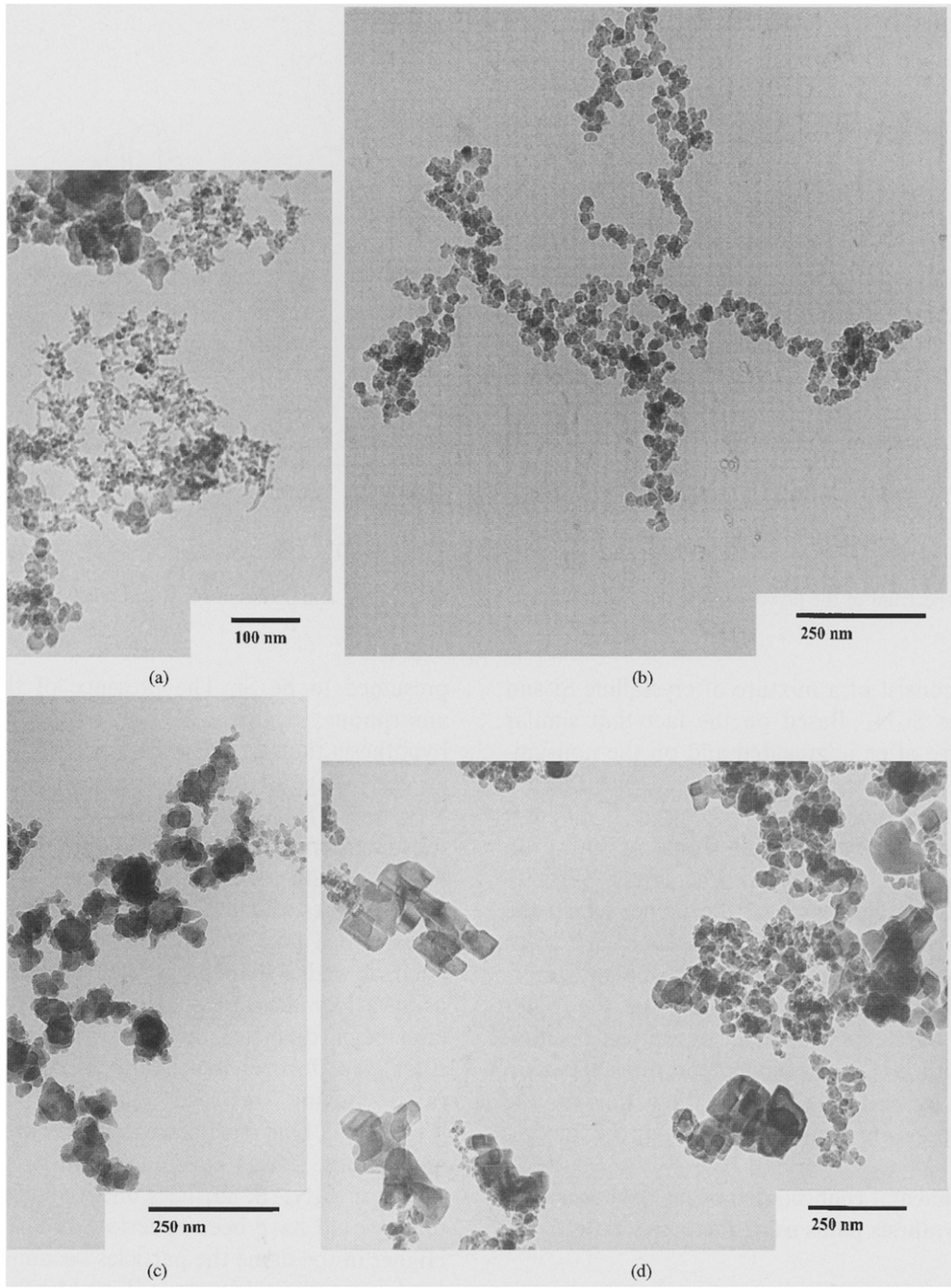

Fig. 11. TEM-photographs of the different types of particles found: (a) small, fibre-like particles, (b) heavily aggregated particles, (c) large, irregular, partially crystalline particles and (d) large, edgy, rectangular, crystalline particles, only found in experiments with increased laser beam diameter.

temperatures into N_2 and H_2. This might also explain why a larger laser beam diameter results in a higher nitrogen-content: the decreased intensity results in less NH_3 decomposition. Therefore, it is essential to obtain the formation of Si_3N_4 before reaching the very high temperatures. When it has been formed, it will not decompose because of the short residence time and it will sinter to larger sizes. On the other hand, when the NH_3 decomposes before the Si_3N_4 starts to form, Si_3N_4 formation is improbable as N_2 is not as reactive as the NH_3. The importance of the mixing in the first process stage is still clearer when comparing these results with those of the premixed case: amorphous particles of 8 nm.[8] Mixing just below the flame, at temperatures where silicon diimide is not present, produces the desired Si_3N_4 particles. For the premixed case, it is not known whether transformation of $Si(NH)_2$ into Si_3N_4 can take place on a millisecond basis, and probably interferes with the sintering process. The experimental results show also that with a carefully designed reactor, the NH_3/SiH_4 ratio needed can be decreased from 15 in an injection mixing reactor,[8] to 4.

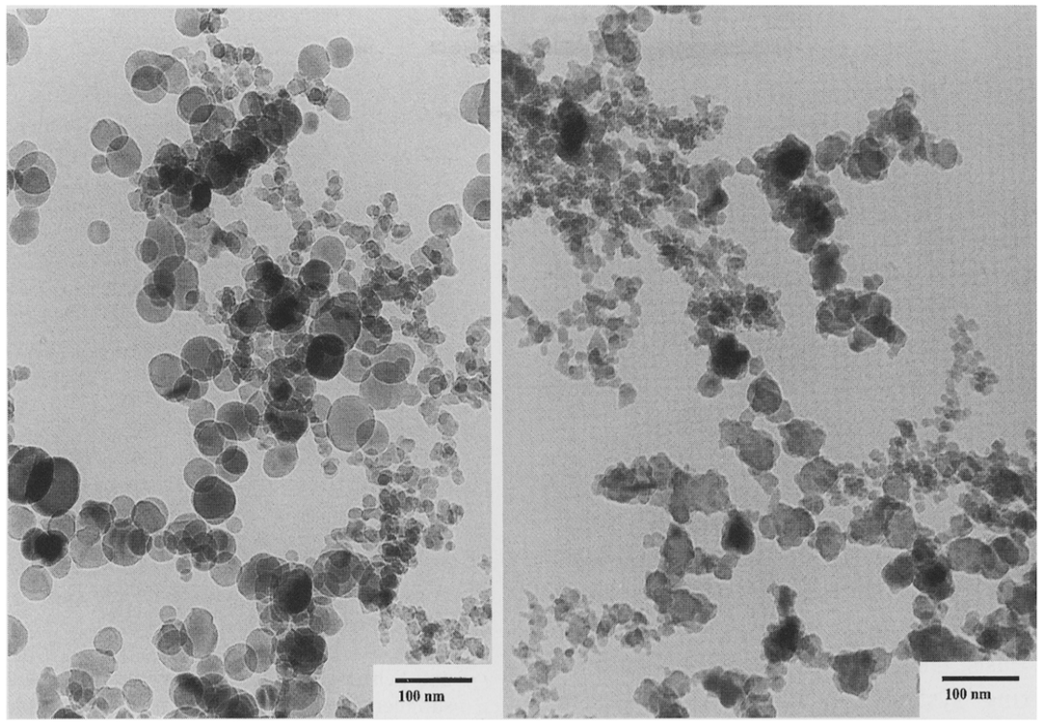

Fig. 12. TEM photographs of particles collected using thermophoretic sampling. Experimental conditions: 100 sccm SiH_4, 200 sccm N_2 sheath-gas, 300 sccm NH_3 and a laser beam diameter of 1·5 mm. The particles are collected at (a) 4 mm and at (b) 9 mm above the nozzle.

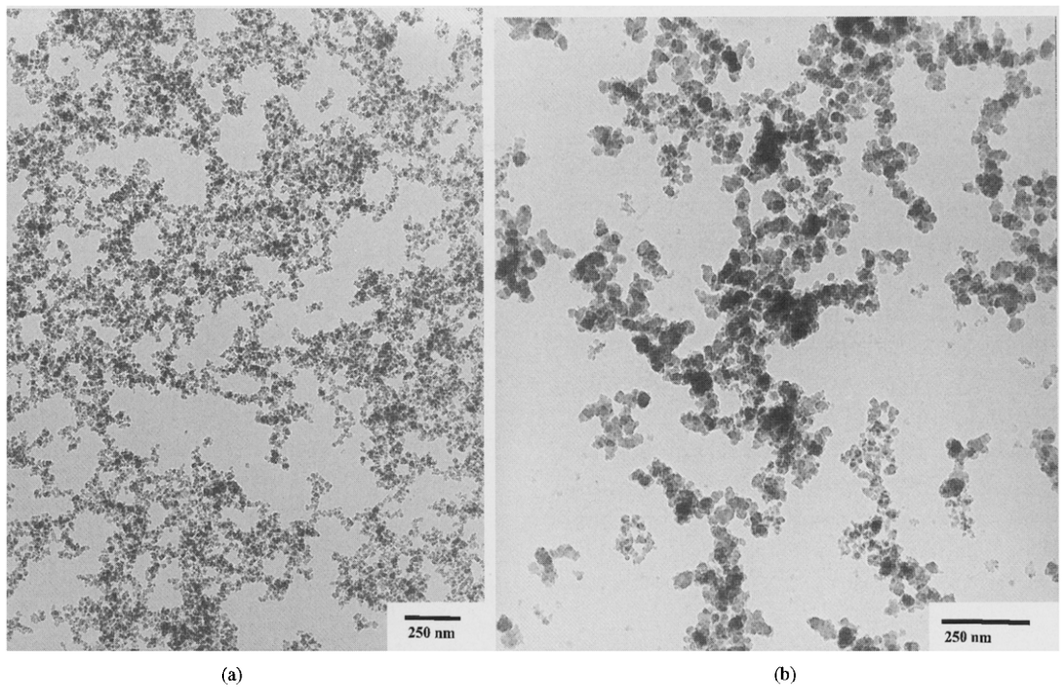

Fig. 13. TEM photographs of particles collected using thermophoretic sampling. Experimental conditions: 80 sccm SiH_4, 40 sccm N_2 sheath-gas, 320 sccm NH_3, and a laser beam diameter of 3·5 mm. The particles are collected at (a) 2 mm and at (b) 8·5 mm above the nozzle.

The two synthesis paths described here both have advantages and disadvantages. Spherical, narrow-distributed Si_3N_4 can probably only be obtained by first producing liquid Si particles with the L-CVP process and eliminating the boundary effects which produce the smaller, more aggregated particles. Then, in a second stage before which the Si aerosol has to be diluted to prevent agglomerate formation, the nitridation of Si with NH_3 must take place at temperatures where the NH_3 does not decompose and where fast nitridation can still take place. The second route, shown here, produces aggregated and non-spherical particles. But stoichiometry, crystallinity, and specific surface area

show favourable properties for sintering. Here also the elimination of the smaller aggregates is important, and needs further optimization.

4 Conclusions

Experimental investigation of SiH_4 pyrolysis in the L-CVP reactor revealed that non-uniform conditions in the flame can lead to a Si powder composed of particles with different sizes and state of aggregation. In order to obtain spherical, non-agglomerated particles the residence time of the Si particles above the melting point (1680 K) must be such as to obtain by coalescence a size for which the sintering is too slow to be of importance. A thermophoretic sampling system enables detection of changes in particle size and morphology on a millisecond basis. Using a newly developed laminar coaxial mixing system for achieving controlled mixing between the reactants SiH_4 and NH_3, two mechanisms for Si_3N_4 formation are found. When the mixing between the SiH_4 and the NH_3 is slow, spherical liquid Si particles are first formed and subsequently nitrided. The powder is however not fully nitrided and contains crystalline Si and amorphous Si_3N_4, probably due to the premature decomposition of the NH_3 due to the high temperatures. When the mixing is such that the SiH_4 and the NH_3 mix below the flame, small amorphous, aggregated Si_3N_4 particles are found low in the flame which subsequently sinter into larger particles higher in the flame. Crystalline (α and β) Si_3N_4 is formed during the cooling of the particle-gas stream above the flame, without contaminating Si. As the flame temperature is between 2000 and 3000 K, where Si_3N_4 is at 1 bar N_2 thermodynamically no longer stable, it was found here that if the Si_3N_4 is formed before it reaches the decomposition temperature, it will not decompose because of the very short residence time at these temperatures.

References

1. Saito, S., *Fine Ceramics*. Elsevier, London, 1988.
2. Lange, F. F. and Kellett, B. J., Thermodynamics of densification:I, sintering of simple particle arrays, equilibrium configurations, pore stability, and shrinkage, II, grain growth in porous compacts and relation to densification. *J. Am. Ceram. Soc.*, 1989, **72**, 725–741.
3. Janiga, J., Sin, K. P. and Figusch, V., Synthesis of silicon nitride powders bygas-phase reaction. *J. European Ceram. Soc.*, 1991, **8**, 153–160.
4. Prochazka, S. and Greskovich, C., Synthesis and characterization of pure silicon nitride powder. *Am. Ceram. Soc. Bull.*, 1978, **57**, 579–581, 586.
5. Cannon, W. R., Danforth, S. C., Flint, J. H., Haggerty, J. S. and Marra, R. A., Sinterable ceramic powders from laser-driven reactions: I, process description and modeling. *J. Am. Ceram. Soc.*, 1982, **65**, 324–330.
6. Cannon, W. R., Danforth, S. C., Haggerty, J. S. and Marra, R. A., Sinterable powder from laser-driven reactions: II, powder characteristcs and process variables. *J. Am. Ceram. Soc.*, 1982, **65**, 330–335.
7. Bauer, R. A., Becht, J. G. M., Kruis, F. E., Scarlett, B. and Schoonman, J., Laser synthesis of low-agglomerated submicrometer silicon nitride powders from chlorinated silanes. *J. Am. Ceram. Soc.*, 1991, **74**, 2759–2768.
8. Aoki, M., Kogyo, T. N., Flint, J. H. and Haggerty, J. S., Synthesis of non-agglomerated Si_3N_4 powder. In *Ceramic Transactions*, Vol. 1A, ed. G. L. Messing, E. R. Fuller and H. Hausner. American Ceramic Society, Westerville, OH, 1988, pp. 150–160.
9. Flint, J. H., Marra, R. A. and Haggerty, J. S., Powder temperature, size and number density in laser driven reactions. *Aerosol Sci. Technol.*, 1986, **5**, 249–261.
10. Dobbins, R. A. and Megaridis, C. M., Morphology of flame-generated soot as determined by thermophoretic sampling. *Langmuir*, 1987, **3**, 254.
11. Hurd, A. J. and Flower, W. L., In situ growth and structure of fractal silica aggregates in a flame. *J. Colloid Interface Sci.*, 1988, **122**, 178.
12. Waltmann, L. and Schmitt, C. M., *Aerosol Science*. Academic Press, London, 1966.
13. Hinds, W. C., *Aerosol Technology*. Wiley, New York, 1982.
14. Kruis, F. E., Kusters, K. A., Pratsinis, S. E. and Scarlett, B., A simple model for the evolution of the characteristics of aggregate particles undergoing coagulation and sintering. *Aerosol Sci. and Technology*, 1993, **19**, 514–526.
15. Kruis, F. E., Scarlett, B., Bauer, R. A. and Schoonman, J., Thermodynamic calculations on the chemical vapor deposition of silicon nitride and silicon from silane and chlorinated silanes. *J. Am. Ceram. Soc.*, 1992, **75**(3), 619–628.